

Efficient Discovery of Selective Small Molecule Agonists of Estrogen-Related Receptor γ using Combinatorial Approach

Yongju Kim,[†] Minseob Koh,[†] Don-Kyu Kim,[§] Hueng-Sik Choi,[§] and Seung Bum Park^{*,†,‡}

Department of Chemistry and Department of Biophysics and Chemical Biology, College of Natural Science, Seoul National University, Seoul 151-747, Korea, and Hormone Research Center, School of Biological Sciences and Technology, Chonnam National University, Gwangju 500-757, Korea

Received May 19, 2009

With the goal of discovering a selective agonist of estrogen-related receptor γ (ERR γ) with enhanced potency, we designed a series of small-molecule ligands derived from a known ERR γ agonist, GSK4716, that can substantially potentiate the transcriptional activity of ERR γ . Individual compounds among a 30-member library of acyl hydrazones were pre-evaluated through *in silico* docking studies on the receptor cavities of ERR γ LBDs using X-ray crystal structures cocrystallized with GSK4716 and 4-OHT. This rational approach to achieve the enhanced potency in ERR γ transcriptional activity with selectivity over ERR α/β enables us to complete the construction of a focused library by carrying out microwave-assisted parallel synthesis with excellent yields and purities. Finally, we identified a more potent ERR γ agonist, **E6**, with excellent selectivity over ERR α/β .

Introduction

Nuclear receptors (NRs) play pivotal roles in activating gene transcription for the embryonic development, growth, differentiation, metabolism, reproduction, homeostasis, and morphogenesis of higher organisms and humans.¹ Most NR ligands are hydrophobic, lipid-soluble, and small in size.² Endogenous ligands for NRs include various cholesterol derivatives, such as steroid hormones, vitamin D, bile acids, retinoids (active forms of vitamin A), and thyroid hormones (modified amino acids). Several members of the nuclear receptor family are classified as orphan nuclear receptors because of the lack of known endogenous or synthetic ligands.³ Estrogen receptor-related receptors (ERRs) are orphan nuclear receptors that are closely related to estrogen receptors (ER α and ER β). Thus far, three isoforms of ERRs (ERR α , ERR β , and ERR γ) have been identified.⁴ Though they share structural homology and sequence similarity with estrogen receptors, ERRs do not bind with or respond to estrogens, endogenous ER ligands.⁵ Among the members of the ERR family, ERR γ is the newest member of the subfamily and is a constitutively active nuclear receptor.⁶ ERR γ is highly expressed in a number of adult human and mouse tissues, including tissues in the brain, skeletal muscle, heart, kidney, pancreas, and placenta.⁷ ERR γ is also expressed in several human fetal tissues, including tissues in the placenta, brain, heart, skeletal muscle, kidney, and lung. Although little is known about its *in vivo* functions, the ERR γ -positive status in breast cancer cells may indicate a favorable prognosis in human breast cancer.⁸ The discovery of selective small-molecule

ligands that would pharmacologically modulate the biological activity of orphan NRs and be utilized as a powerful tool for elucidating the biological roles of these receptors is a breakthrough in the study of biological function of orphan NRs. Because of its potential roles in cancers and metabolic disease, ERR γ has attracted significant attention from the scientific community for the discovery of novel ligands. Recently, 4-hydroxytamoxifen (4-OHT) and diethylstilbestrol (DES), known as antagonist and agonist of ER α , respectively, were reported as inverse agonists of ERR β and ERR γ . This was confirmed by biochemical and X-ray crystallographic studies.⁹ In addition, phenolic acyl hydrazones were reported as functional ERR γ agonists, although *in-depth* studies of its molecular basis and the observed agonistic response were not carried out.¹⁰ Because of the limited selectivity and specificity of the reported ligands, selective small-molecule ligands for ERR γ have to be obtained for the fundamental understanding of the biological roles of ERR γ .

Under this condition, we aimed to discover novel and selective ERR γ ligands by a rational design along with biomedical analysis and computational docking simulation. In fact, the rational design of small-molecule ligands having the desired selectivity is still far from being achieved because of the complexity of underlying biological phenomena; further, the discovery of small-molecule ligands has been pursued with limited predictability in a low-throughput manner. Therefore, we decided to use an empirical combinatorial approach to significantly enhance the efficiency in synthesis and compensate the limited predictability in rational design.

Results and Discussion

With the goal of discovering a selective ligand of ERR γ , we analyzed the selectivity, affinity, and functional activity

* To whom correspondence should be addressed. Tel: +82-2-880-9090. Fax: +82-2-884-4025. E-mail: sbpark@snu.ac.kr.

[†] Department of Chemistry, Seoul National University.

[‡] Department of Biophysics and Chemical Biology, Seoul National University.

[§] Hormone Research Center, Chonnam National University.

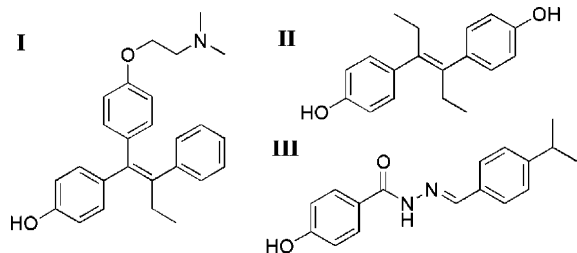


Figure 1. Reported ligands of ERRs. **I.** 4-OHT: Synthetic antagonist of ER α and inverse agonist of ERR γ . **II.** DES: Synthetic agonist of ER α and inverse agonist of ERR γ . **III.** GSK 4716: Synthetic agonist of ERR β/γ .

of known ligands. When we compared X-ray crystal structures of ERR γ ligand binding domains (LBDs) cocrystallized with GSK4716 and 4-OHT,¹¹ respectively, we identified the key difference in their interactions in molecular levels at the binding pockets, which might be exploited for the improvement of affinity and selectivity toward ERR γ . As shown in Figure 2a, 4-OHT, a synthetic antagonist of ER α and an inverse agonist of ERR γ , resides mainly in pocket B, and the phenol part of 4-OHT has intact hydrogen bonding with Arg316 and Asp275 at the binding pocket of LBDs. In fact, these two residues serve as gatekeepers by narrowing the hole toward pocket A. In comparison, the phenolic OH group on an aryl ring of GSK4716, a selective agonist of ERR β/γ , but not a ligand for ER α/β , has a specific interaction with Asp328 as the deep binding pocket (pocket A), and GSK4716 is accommodated throughout pockets A and B. This results from the rearrangement of the gatekeeper residues (Arg316 and Asp275) of LBD (see Figure 2b). When we overlapped the two binding pockets of ERR γ LBDs cocrystallized with 4-OHT and GSK4716, respectively, we could conclude that the selectivity of GSK4716 toward ERR β/γ over ER α/β was caused by the deep penetration at the binding pocket of the ERR γ LBD. In particular, we found that the phenol part of 4-OHT and isopropylbenzene part of GSK 4716 lie nicely on top of each other in the crystal structures of the 4-OHT- and GSK4716-bound ERR γ LBDs (see Figure 2c). On the basis of this analysis, we could further improve the selectivity of GSK4716 toward ERR γ through the introduction of selectivity elements at pocket B along with the deep penetration at pocket A for specific hydrogen bonding with Asp328, as well as the interaction of a hydrazone moiety with gatekeeper residues. Therefore, the enhanced stabilization of ligands at the ERR γ LBD can ultimately lead to the specific agonist of ERR γ with enhanced affinity over classic ERs. The schematics of the elements used for the selective ERR γ agonist are shown in Figure 2d.

On the basis of this molecular skeleton with an acyl hydrazone moiety derived from computational analysis, we designed and prepared a series of R¹ substituents with hydrazide moieties and R² substituents with benzaldehyde moieties to enhance the binding affinity to ERR γ . Upon condensation by microwave irradiation, the two reactants react to afford the final compounds via the efficient formation of a hydrazone moiety at the linker region.

First, hydrazide building blocks were designed to maximize the efficient hydrogen bondings with Asp328. Therefore, R¹ substituents were incorporated with aryl or heteroaryl

moieties containing a hydroxy or amino group (Scheme 1). Hydrazides **A** and **D** were directly borrowed from previously reported compounds.¹⁰ The crystal structure of GSK4716-bound ERR γ LBD reveals that the C(3) atom of GSK4716 hydrazide is adjacent to the amide N–H of the peptide backbone of Asp328 and the ϵ -amino group of Lys248 with distances of 3.8 Å and 4.7 Å, respectively, suggesting that the introduction of a hydrogen bonding element at the C(3) position of an aryl moiety on the hydrazide building blocks might induce additional hydrogen bonding at the binding pocket and enhance affinity and selectivity to ERR γ . In order to test our hypothesis, we designed and synthesized hydrazide building blocks **B**, **C**, and **E** through the exchange of the C(3) atom with nitrogen to introduce pyridine (**B**, **E**) and pyridone (**C**). The hydrazide building blocks were synthesized with excellent yield and purity through a microwave-assisted nucleophilic acyl substitution reaction of methyl ester with hydrazine (see Supporting Information).

Aldehyde building blocks with R² substituents were designed to maximize the selective interaction of small-molecule ligands at pocket B along with the synergistic binding at the deep binding pocket A on the binding site of the ERR γ LBD. As shown in Scheme 2, aldehyde building blocks **1** and **2** were directly borrowed from previously reported building blocks.¹⁰ Aldehydes **3** and **4** with the DES and 4-hydroxytamoxifen moiety, respectively, were designed to introduce tighter binding at pocket B of the ERR γ LBD. In fact, the size of pocket B at the GSK4716-bound ERR γ LBD is much smaller than the size of that at the 4-OHT-bound ERR γ LBD, probably because of the induced fit of the protein. To compensate for this reduced space at the binding pocket with specificity, we designed trimmed moieties of DES and 4-OHT, such as stilbene and its isostere, azobenzene for aldehyde building blocks **5** and **6**, respectively. Aldehyde building blocks **1**, **2**, and **5** are commercially available, but aldehydes **2**, **3**, and **6** were prepared in-house using the synthetic routes shown in Scheme 3. McMurry coupling between **7** and propiophenone produced **8** (*E/Z* = 3.2:1), and subsequently, LiAlH₄ (LAH) reduction, followed by Dess–Martin periodinone (DMP) oxidation, yielded the desired aldehyde building block **3**. Aldehyde **4** was synthesized from **9** through a series of reactions: Mono-protection of **9**, Pd-mediated CO insertion, LAH reduction, DMP oxidation, deprotection, and O-alkylation. Aldehyde **6** was also prepared easily through LAH reduction and DMP oxidation. Finally, we could complete a set of six aldehyde building blocks (see Supporting Information).

For the preliminary evaluation of our designed molecular skeletons, we executed virtual screening by computer-aided docking simulation performed using the Discovery Studio 1.7 program. We utilized previously reported X-ray crystal structures of the GSK4716-bound and 4-OHT-bound ERR γ LBDs (PDB IDs 2GPP and 2GPU, respectively),¹¹ and the individual small molecules were evaluated for their potential binding to receptor cavities of ERR γ LBDs using the LigandFit module implemented with the Receptor–Ligand Interaction (RLI) protocol (see Supporting Information for the detailed procedure). The dock scores of individual molecules toward two receptor cavities of GSK4716-bound

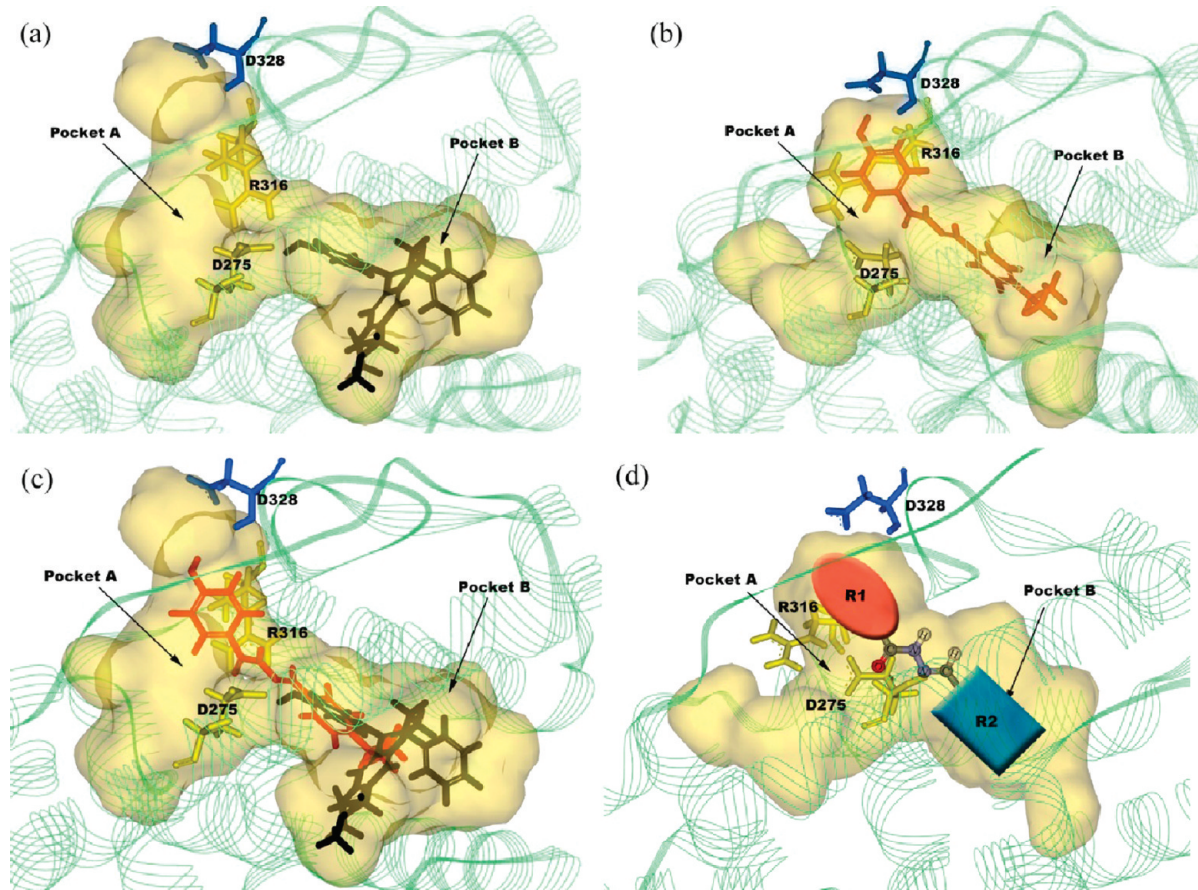
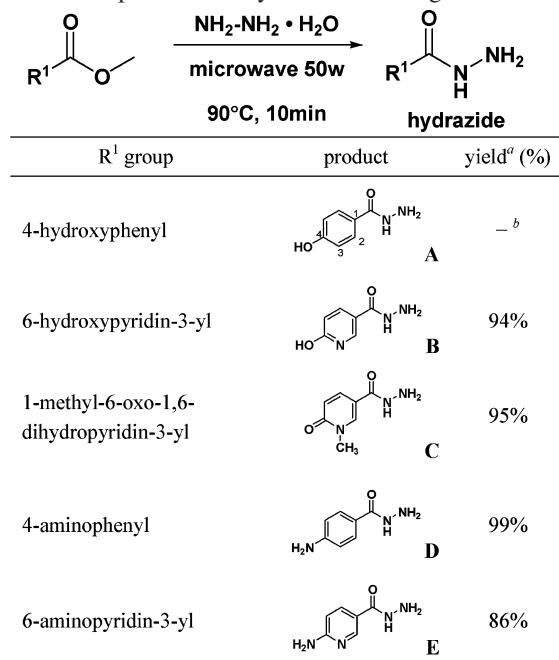


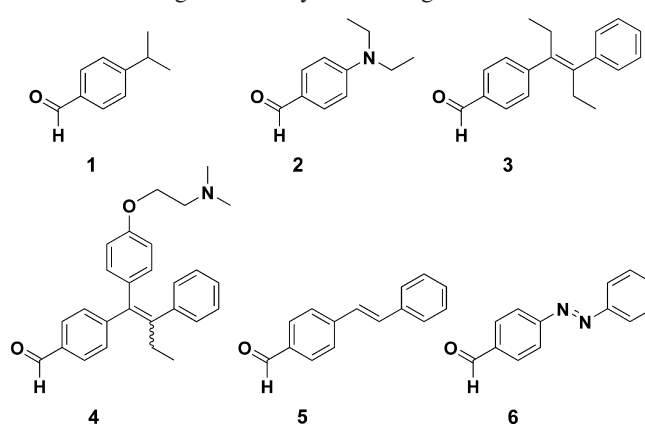
Figure 2. X-ray crystal structures of a ligand-bound ERR γ ligand binding domain (LBD) and schematic illustration of our combinatorial approach for the discovery of selective small-molecule ligands to the ERR γ LBD. (a) 4-Hydroxytamoxifen(4-OHT)-bound LBD of ERR γ (PDB ID 2GPU). (b) GSK4716-bound LBD of ERR γ (PDB ID 2GPP). (c) Overlay of GSK4716 on 4-OHT-bound LBD of ERR γ . (d) Schematic illustration of the designed template used in our combinatorial approach at LBD of ERR γ (PDB ID 2GPP).

Scheme 1. Preparation of Hydrazone Building Blocks^{a,b}



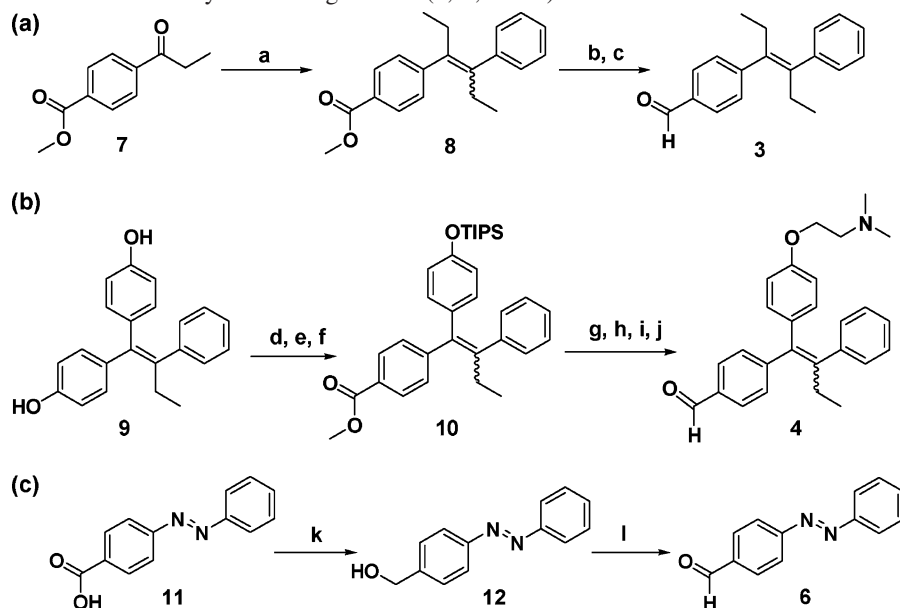
^a Isolated yield. ^b Commercially available.

Scheme 2. Design of Aldehyde Building Blocks



with similar molecular skeletons to GSK4716 were fitted nicely to the binding pocket of the ERR γ LBD that is derived from the GSK4716-bound crystal structure (PDB ID 2GPP), whereas the other ligands with bulkier substituents at the R² position did not fit the binding pocket, particularly pocket B. In fact, for compounds with aldehydes **5** and **6**, reasonable binding events were observed at the receptor cavity of the GSK4716-bound ERR γ LBD. In the case of the docking study involving the receptor cavity of the 4-OHT-bound ERR γ LBD (PDB ID 2GPU), we did not observe any significant binding events because of the tight arrangement of gatekeeper residues (Arg316 and Asp275) between

and 4-OHT-bound ERR γ LBDs are summarized in Tables S1 and S2, Supporting Information. As expected, the ligands

Scheme 3. Synthetic Methods for Aldehyde Building Blocks (**3**, **4**, and **6**)^a

^a Reagents and conditions: (a) propiophenone, TiCl₄, Zn, THF, microwave, 70 °C, 40 min, 65% (*E/Z* = 3.2:1); (b) LAH, THF, rt, 2 h, 95%; (c) Dess–Martin periodinane, DCM, rt, 2 h, 95%; (d) TIPSCl, imidazole, DCM, 0 °C → rt, 74%; (e) Tf₂O, 2,6-lutidine, DMAP, DCM, 0 °C → rt, 5 h; (f) CO (5 atm), Pd(OAc)₂, dppp, TEA, MeOH/DMF, 70 °C, 20 h, 67%; (g) LAH, THF, rt, 2 h, 97%; (h) Dess–Martin periodinane, DCM, rt, 2 h, 95%; (i) TBAF, THF, rt, 2 h, 92%; (j) 2-chloro-*N,N*-dimethylethanamine, Cs₂CO₃, DMF, microwave, 80 °C, 78%; (k) LAH, THF, rt, 2 h, 62%; (l) Dess–Martin periodinane, DCM, rt, 2 h, 77%.

pockets A and B of the LBD. Although we did not achieve the systematic pattern of prediction for the selective binding events on the receptor cavities of ERR γ LBDs, we witnessed slight indication of the potential selectivity for the discovery of novel ligands for ERR γ through the introduction of the bulkier residue at the R² position in our modified skeleton.

After the preparation of hydrazide (A–E) and aldehyde (1–6) building blocks, we synthesized a series of acyl hydrazone compounds through microwave-assisted solution phase parallel synthesis for the discovery of more potent small-molecule ligands of ERR γ . Scheme 4 shows the structures of the final acyl hydrazones along with their synthetic yields. The microwave-assisted condensation of hydrazide and aldehyde in *n*-BuOH provided excellent yields and purities of acyl hydrazone with a significant enhancement in the reaction rates compared to conventional thermal reactions. The identity of each of the final compounds was confirmed by ¹H/¹³C NMR and mass spectrometry (see Experimental Section and Supporting Information).

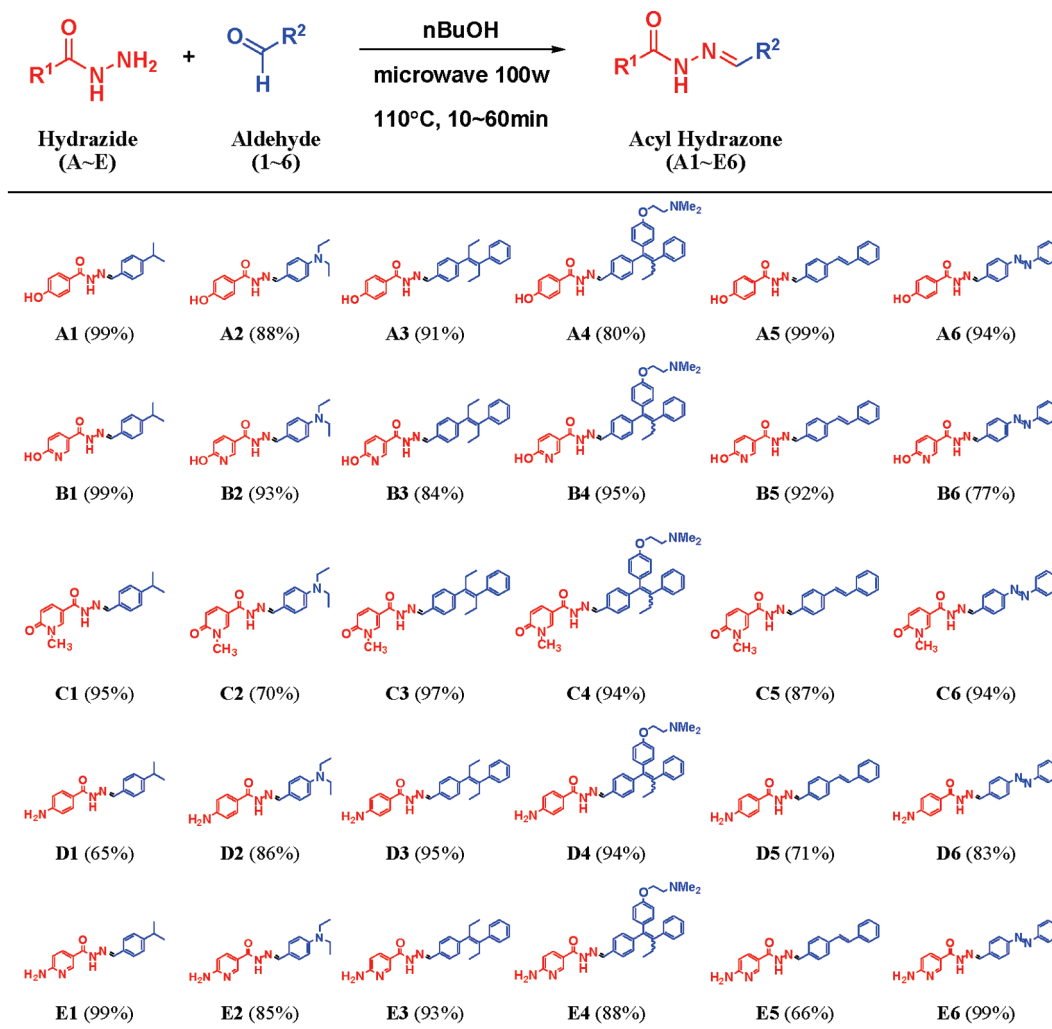
Upon the completion of the full matrix with the 30-member focused library of acyl hydrazones, we pursued the biological evaluation of the resulting compound collection using a cell-based reporter-gene assay to monitor the regulation of the transcriptional activity of ERR γ upon the treatment of small-molecule ligands. A mammalian one-hybrid assay was performed in COS-1 cells using transient transfection with a vector expressing the ligand binding domain (LBD) of ERR γ fused to the Gal4 DNA binding domain (DBD) and a reporter plasmid containing five Gal4 binding sites upstream of the firefly luciferase gene in the pGL2 vector. We used GSK 4716 as a known ERR γ agonist and 4-OHT as a known ERR γ inverse agonist to compare the constitutive activity of unliganded ERR γ . Many compounds of this focused library showed similar activities at

the 1 μ M concentration to those of GSK4716, probably due to their shared pharmacophore, acyl hydrazone.¹⁰ We were pleasantly surprised to find that **E6** significantly enhanced the transcriptional activity of ERR γ in the cell-based reporter-gene assay system in COS-1 cells (see Figure 3). As we discussed in our previous *in silico* analysis, **E6** was speculated to be accommodated at the binding cavity of the ERR γ LBD both at pockets A and B through the induced fit, which might lead to its selective agonism on ERR γ but not on ERR α and β (see Figure 4 and Supporting Information).

The excellent potency of **E6** for the transcriptional activity of ERR γ encouraged us to further investigate the biological functions of **E6**, along with its selectivity toward ERR α , β , and γ . For verifying its selectivity toward ERR γ over ERR α and β , the LBD regions of ERR α and β were PCR-amplified in the same plasmid construct (pGL2 vector) used in ERR γ . As shown in Figure 5, **E6** serves as a potent agonist of ERR γ and shows transcriptional activity, even at a 10 nM concentration and the efficacy of **E6** at this concentration was comparable to that of the leading agonist, GSK 4716 at 1 μ M concentration. More importantly, **E6** demonstrated the excellent selectivity toward ERR γ without any agonistic effects on ERR α and ERR β .

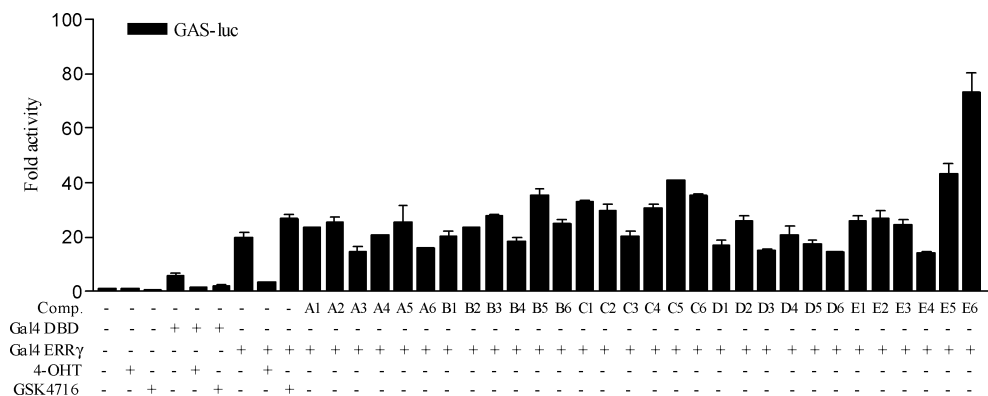
Conclusion

With the goal of discovering a selective agonist of ERR γ with enhanced potency, we designed a series of small-molecule ligands derived from a known ERR γ agonist, GSK4716, that can substantially potentiate the transcriptional activity of ERR γ . Individual compounds among a 30-member library of acyl hydrazones were pre-evaluated through *in-silico* docking studies on the receptor cavities of ERR γ LBDs using X-ray crystal structures cocrystallized

Scheme 4. Combinatorial Synthesis of Acyl Hydrazone Using Condensation between a Hydrazone and Aldehyde

with either GSK4716 or 4-OHT. This rational approach to achieve the enhanced potency in $\text{ERR}\gamma$ transcriptional activity with selectivity over $\text{ERR}\alpha/\beta$ enables us to pursue the design and construction of a focused library by carrying out microwave-assisted parallel synthesis with excellent yields and purities. The biological evaluation of focused library members was pursued through the cell-based reporter-gene assay in COS-1 cells, and we identified a more potent $\text{ERR}\gamma$ agonist, **E6**, with excellent selectivity over $\text{ERR}\alpha/\beta$. Selective $\text{ERR}\gamma$ agonist **E6** discovered in this study is 2 orders of magnitude more potent than the known $\text{ERR}\gamma$

agonist GSK4716. Especially, we would like to emphasize that the systematic combinatorial approach can overcome the limited predictability of in-silico screening with nonflexible docking algorithm. In fact, the new $\text{ERR}\gamma$ agonist **E6** was not predicted as a tight binder toward $\text{ERR}\gamma$. Therefore, we have successfully demonstrated the inevitability and efficiency of interdisciplinary approach comprised of in silico analysis for enhancing the selective binding at the receptor cavity, combinatorial construction of a focused library by carrying out microwave-assisted solution-phase synthesis, and a cell-based reporter gene assay with a panel of $\text{ERR}\alpha/\beta$

**Figure 3.** Cell-based reporter-gene assay data for 30 small-molecule ligands.

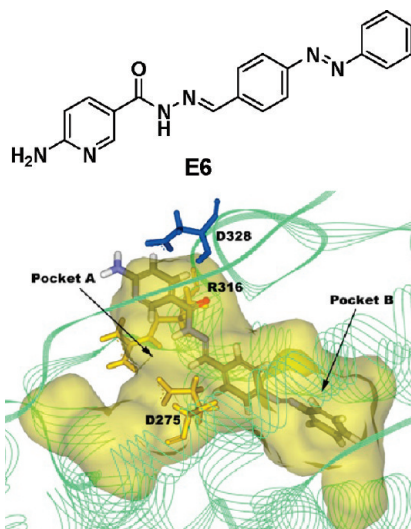


Figure 4. Novel synthetic agonist of ERR γ (**E6**) and the predicted binding mode of **E6** at the binding cavity of ERR γ LBD.

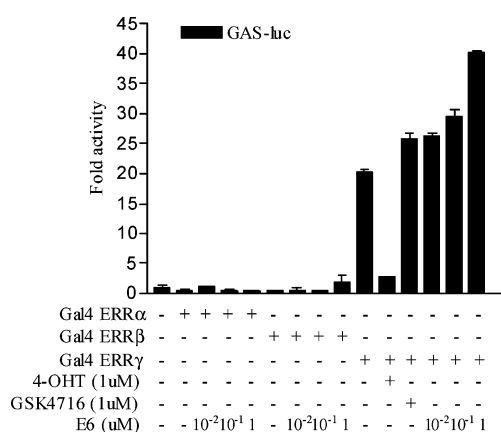


Figure 5. Selectivity of **E6** between ERR α , ERR β , and ERR γ .

β/γ for the discovery of a novel ERR γ agonist. The biological application of the new ERR γ agonist and its mode of action will be reported in due course.

Experimental Section

General Information. All reactions were performed either in oven-dried glassware or microwave vessel under dry argon atmosphere. Toluene and tetrahydrofuran (THF) was dried by distillation from sodium-benzophenone immediately prior to use. Dichloromethane (DCM) was dried by distillation from CaH₂. Other solvent and organic reagent were purchased from commercial vendors and used without further purification unless otherwise mentioned. ¹H and ¹³C NMR spectra were obtained on 300 and 500 MHz FT-NMR spectrophotometer. Chemical shifts were reported in ppm relative to the residual solvent peak for CDCl₃ (¹H, 7.24; ¹³C, 77.23), CD₃OD (¹H, 3.31; ¹³C, 49.15), (CD₃)₂CO (¹H, 2.05; ¹³C, 29.92), and (CD₃)₂SO (¹H, 2.50; ¹³C, 39.51). Multiplicity was indicated as follows: s (singlet), d (doublet), t (triplet), q (quartet), quin (quintet), m (multiplet), dd (doublet of doublet), ddd (doublet of doublet of doublet), dt (doublet of triplet), td (triplet of doublet), br s (broad singlet), etc. Coupling constants were reported in hertz. Routine mass

analyses were performed on LC/MS system equipped with a reverse phase column (C-18, 50 × 2.1 mm, 5 μ m) and photodiode array detector using electron spray ionization (ESI) or atmospheric pressure chemical ionization (APCI). The high resolution mass spectrometric analyses were conducted at the Mass Spectrometry Laboratory of Seoul National University using mass spectrometer by direct injection for fast atomic bombardment (FAB). Microwave reaction was performed using CEM Discover Benchmate and microwave reaction conditions were denoted in Experimental Section. The products were purified by flash column chromatography on silica gel (230–400 mesh). The eluent used for purification is reported in parentheses. Thin-layer chromatography (TLC) was performed on precoated glass-backed plates (silica gel 60 F₂₅₄ 0.25 mm), and components were visualized by observation under UV light (254 and 365 nm) or by treating the plates with anisaldehyde, KMnO₄, phosphomolybdic acid, and vaniline followed by heating. Distilled water was polished by ion exchange and filtration.

Gal4 Fusion Constructs and Transient Transfection Assay. The LBD region of ERR α , β , and γ were PCR amplified using Pfu DNA polymerase and digested with *EcoRI/XhoI* and ligated into *EcoRI/SalI*-digested pCMX-Gal4 DBD.¹² COS-1 cells were maintained in DMEM (Hyclone) supplemented with 10% fetal bovine serum (FBS, Hyclone) and antibiotics (Hyclone) in a humidified atmosphere containing 5% CO₂ at 37 °C. The day before transfection, cells were seeded into 24-well plates at a density of 2–8 × 10⁴ cells/well. Transient transfections were performed along with a reporter construct containing five Gal4 binding sites upstream of the firefly luciferase gene in the pGL2 vector (Promega) using SuperFect (Qiagen) for COS-1, according to the manufacturer's instructions. The cells were treated with 4-OHT, GSK4716, or compounds for final 24 h after transfection. Luciferase activity was measured 48 h after transfection and normalized to β -galactosidase activity.

General Procedure for Synthesis of Acyl Hydrazone A1–E6. To a solution of hydrazide of *n*-BuOH (0.1M) was added aldehyde (1.2 equiv.) and the resulting mixture was heated in capped microwave vessel under microwave irradiation (100 W, 100 °C) for 5–60 min. After reaction was complete as monitored by TLC, the crude product was condensed under reduced pressure without aqueous workup procedure and purified by silica-gel flash column chromatography to provide desired products. Some final compounds, such as **B1**, **B2**, **A5–E5**, and **A6–E6**, were purified by crystallization. The residual starting materials and impurities were removed by simple washing with MeOH and DCM.

Characterization of Compound A1: ¹H NMR (300 MHz, CD₃OD) δ 8.30 (s, 1H), 7.85 (d, *J* = 8.6 Hz, 2H), 7.77 (d, *J* = 8.0 Hz, 2H) 7.33 (d, *J* = 8.1 Hz, 2H), 6.90 (d, *J* = 8.7 Hz, 2H), 3.01–2.92 (m, 1H), 1.29 (d, *J* = 6.9 Hz, 6H); ¹³C NMR (125 MHz, CD₃OD) δ 162.8, 153.1, 150.2, 133.5, 131.0, 129.0, 128.0, 127.9, 125.1, 116.5, 116.4, 35.5, 24.3; LRMS(ESI⁺) *m/z* calcd for C₁₇H₁₉N₂O₂ [M + H]⁺ 283.14; found 283.08.

Characterization of Compound A2: ^1H NMR (300 MHz, CD_3OD) δ 8.17 (s, 1H), 7.82 (d, $J = 8.6$ Hz, 2H), 7.65 (d, $J = 8.7$ Hz, 2H), 6.89 (d, $J = 8.7$ Hz, 2H), 6.73 (d, $J = 8.9$ Hz, 2H), 3.45 (q, $J = 7.0$ Hz, 4H), 1.20 (t, $J = 7.0$ Hz, 6H); ^{13}C NMR (125 MHz, CD_3OD) δ 166.6, 162.6, 151.4, 151.1, 130.8, 130.7, 125.3, 122.3, 116.4, 112.5, 45.5, 13.0; LRMS(ESI^+) m/z calcd for $\text{C}_{18}\text{H}_{22}\text{N}_3\text{O}_2$ [$\text{M} + \text{H}$] $^+$ 312.17; found 312.13.

Characterization of Compound A3: a mixture of stereoisomers ($E/Z = 85:15$); ^1H NMR (300 MHz, acetone- d_6) δ 10.83 (s, $0.85 \times 1\text{H}$), 9.06 (s, $0.85 \times 1\text{H}$), 7.93 (d, $J = 8.6$ Hz, $0.15 \times 2\text{H}$), 7.88 (d, $J = 8.6$ Hz, $0.85 \times 2\text{H}$), 7.78 (d, $J = 7.9$ Hz, $0.15 \times 2\text{H}$), 7.44 (d, $J = 8.0$ Hz, $0.85 \times 2\text{H}$), 7.39 (d, $J = 7.7$ Hz, $0.15 \times 2\text{H}$), 7.33–7.25 (m, $0.15 \times 5\text{H}$), 7.10–6.91 (m, 9H), 2.65–2.56 (m, $0.85 \times 4\text{H}$), 2.21–2.14 (m, $0.15 \times 4\text{H}$), 0.99–0.93 (m, $0.85 \times 6\text{H}$), 0.80–0.75 (m, $0.15 \times 6\text{H}$); ^{13}C NMR (75 MHz, acetone- d_6) δ 161.6, 146.1, 143.9, 140.9, 139.7, 133.3, 131.1, 130.6, 130.1, 129.6, 129.1, 128.5, 128.0, 127.3, 126.7, 125.9, 116.0, 28.0, 27.7, 13.7, 13.6; LRMS(APCI $^+$) m/z calcd for $\text{C}_{26}\text{H}_{27}\text{N}_2\text{O}_2$ [$\text{M} + \text{H}$] $^+$ 399.21; found 399.10.

Characterization of Compound A4: a mixture of stereoisomers ($E/Z = 46:54$); ^1H NMR (500 MHz, CD_3OD) δ 8.34 (s, $0.54 \times 1\text{H}$), 8.14 (s, $0.46 \times 1\text{H}$), 7.85 (d, $J = 8.5$ Hz, $0.54 \times 2\text{H}$), 7.80–7.78 (m, 2H), 7.42 (d, $J = 8.0$ Hz, $0.46 \times 2\text{H}$), 7.24 (d, $J = 8.5$ Hz, $0.54 \times 2\text{H}$), 7.25–7.06 (m, $0.54 \times 5\text{H}$, $0.46 \times 9\text{H}$), 6.92 (d, $J = 8.5$ Hz, $0.46 \times 2\text{H}$), 6.88 (d, $J = 8.5$ Hz, $0.54 \times 2\text{H}$), 6.85 (d, $J = 8.5$ Hz, $0.46 \times 2\text{H}$), 6.75 (d, $J = 9.0$ Hz, $0.54 \times 2\text{H}$), 6.56 (d, $J = 9.0$ Hz, $0.54 \times 2\text{H}$), 4.09 (t, $J = 5.3$ Hz, $0.46 \times 2\text{H}$), 3.91 (t, $J = 5.5$ Hz, $0.54 \times 2\text{H}$), 2.77 (t, $J = 5.2$ Hz, $0.46 \times 2\text{H}$), 2.67 (t, $J = 5.2$ Hz, $0.54 \times 2\text{H}$), 2.51–2.43 (m, 2H), 2.34 (s, $0.46 \times 6\text{H}$), 2.27 (s, $0.54 \times 6\text{H}$), 0.93–0.89 (m, 3H); ^{13}C NMR (125 MHz, CD_3OD) δ 166.96, 166.85, 163.4, 163.3, 159.2, 158.4, 149.8, 149.7, 147.4, 147.2, 144.4, 143.6, 143.5, 143.5, 139.5, 139.4, 137.0, 136.7, 134.2, 133.2, 133.1, 132.4, 131.9, 131.09, 131.05, 130.99, 130.95, 129.2, 129.1, 128.8, 127.9, 127.6, 127.4, 124.48, 124.46, 116.63, 116.58, 115.4, 114.7, 66.6, 66.3, 59.2, 59.1, 45.93, 45.86, 30.2, 30.1, 14.09, 14.05; LRMS(ESI^+) m/z calcd for $\text{C}_{34}\text{H}_{36}\text{N}_3\text{O}_3$ [$\text{M} + \text{H}$] $^+$ 534.28; found 534.11.

Characterization of Compound A5: ^1H NMR (500 MHz, DMSO- d_6) δ 10.12 (s, 1H), 8.41 (s, 1H), 7.80 (d, $J = 8.0$ Hz, 2H), 7.69 (br m, 4H), 7.63 (d, $J = 7.5$ Hz, 2H), 7.40–7.28 (m, 5H), 6.86 (d, $J = 8.0$ Hz, 2H); ^{13}C NMR (125 MHz, DMSO- d_6) δ 162.7, 160.6, 146.4, 138.5, 136.9, 133.7, 129.6, 129.4, 128.7, 127.83, 127.78, 127.3, 126.8, 126.6, 123.9, 115.0; LRMS(ESI^+) m/z calcd for $\text{C}_{22}\text{H}_{19}\text{N}_2\text{O}_2$ [$\text{M} + \text{H}$] $^+$ 343.14; found 343.09.

Characterization of Compound A6: ^1H NMR (500 MHz, DMSO- d_6) δ 11.83 (br s, 1H), 10.17 (s, 1H), 8.52 (br s, 1H), 7.98–7.91 (m, 6H), 7.85 (d, $J = 8.5$ Hz, 2H), 7.63–7.58 (m, 3H), 6.89 (d, $J = 8.6$ Hz, 2H); ^{13}C NMR (125 MHz, DMSO- d_6) δ 162.4, 160.5, 152.4, 152.0, 145.8, 139.2, 138.2, 137.2, 131.9, 129.6, 128.1, 123.2, 122.7, 119.5, 111.0; LRMS(APCI $^+$) m/z calcd for $\text{C}_{20}\text{H}_{17}\text{N}_4\text{O}_2$ [$\text{M} + \text{H}$] $^+$ 345.14; found 345.20.

Characterization of Compound B1: ^1H NMR (500 MHz, DMSO- d_6) δ 11.93 (br s, 1H), 11.46 (s, 1H), 8.31 (br s, 1H),

8.14 (s, 1H), 7.92 (dd, $J = 9.5, 3.0$ Hz, 1H), 7.61 (d, $J = 8.5$ Hz, 2H), 7.32 (d, $J = 8.5$ Hz, 2H), 6.40 (d, $J = 9.5$ Hz, 1H), 2.93 (quin, $J = 6.9$ Hz, 1H), 1.22 (d, $J = 7.0$ Hz, 6H); ^{13}C NMR (125 MHz, DMSO- d_6) δ 162.3, 160.3, 146.4, 150.6, 147.1, 139.2, 137.9, 132.0, 127.1, 126.8, 119.4, 111.2, 33.4, 23.7; LRMS(ESI^+) m/z calcd for $\text{C}_{22}\text{H}_{19}\text{N}_2\text{O}_2$ [$\text{M} + \text{H}$] $^+$ 343.14; found 343.09.

Characterization of Compound B2: ^1H NMR (500 MHz, DMSO- d_6) δ 12.03 (br s, 1H), 11.29 (s, 1H), 8.18 (s, 1H), 8.08 (s, 1H), 7.90 (d, $J = 9.0$ Hz, 1H), 7.48 (d, $J = 8.5$ Hz, 2H), 6.69 (d, $J = 9.0$ Hz, 2H), 6.39 (d, $J = 9.5$ Hz, 1H), 3.38 (q, $J = 9.0$ Hz, 4H), 1.10 (d, $J = 7.0$ Hz, 6H); ^{13}C NMR (125 MHz, DMSO- d_6) δ 162.2, 159.8, 148.8, 148.0, 139.1, 137.5, 128.6, 120.6, 119.2, 111.5, 111.1, 43.7, 12.4; LRMS(APCI $^+$) m/z calcd for $\text{C}_{17}\text{H}_{21}\text{N}_4\text{O}_2$ [$\text{M} + \text{H}$] $^+$ 313.17; found 313.06.

Characterization of Compound B3: ^1H NMR (500 MHz, DMSO- d_6) δ 12.04 (br s, 1H), 11.53 (s, 1H), 8.21 (s, 1H), 8.10 (s, 1H), 7.89 (dd, $J = 9.5, 20$ Hz, 1H), 7.40 (d, $J = 6.5$ Hz, 2H), 7.10–6.94 (m, 7H), 6.39 (d, $J = 9.5$ Hz, 1H), 2.56–2.52 (m, 4H), 0.94–0.89 (m, 6H); ^{13}C NMR (75 MHz, DMSO- d_6) δ 162.2, 144.6, 142.4, 139.4, 138.1, 131.6, 129.9, 129.4, 127.6, 126.2, 125.8, 119.3, 119.1, 111.1, 26.9, 26.5, 13.2, 13.1; LRMS(APCI $^+$) m/z calcd for $\text{C}_{25}\text{H}_{26}\text{N}_3\text{O}_2$ [$\text{M} + \text{H}$] $^+$: 400.20; Found: 400.08.

Characterization of Compound B4: a mixture of stereoisomers ($E/Z = 46:54$); ^1H NMR (500 MHz, CD_3OD) δ 8.30 (s, $0.54 \times 1\text{H}$), 8.22 (s, $0.54 \times 1\text{H}$), 8.17 (s, $0.46 \times 1\text{H}$), 8.11 (s, $0.46 \times 1\text{H}$), 8.09 (d, $J = 9.5$ Hz, $0.54 \times 1\text{H}$), 8.04 (d, $J = 9.5$ Hz, $0.46 \times 1\text{H}$), 7.82 (d, $J = 8.0$ Hz, $0.54 \times 2\text{H}$), 7.45 (d, $J = 8.0$ Hz, $0.46 \times 2\text{H}$), 7.30 (d, $J = 8.0$ Hz, $0.54 \times 2\text{H}$), 7.19–7.09 (m, $0.54 \times 5\text{H}$, $0.46 \times 7\text{H}$), 6.97 (d, $J = 9.0$ Hz, $0.46 \times 2\text{H}$), 6.93 (d, $J = 8.5$ Hz, $0.46 \times 2\text{H}$), 6.78 (d, $J = 8.5$ Hz, $0.54 \times 2\text{H}$), 6.60 (d, $J = 8.5$ Hz, $0.54 \times 2\text{H}$), 6.59–6.55 (m, 1H), 4.14 (t, $J = 5.5$ Hz, $0.46 \times 2\text{H}$), 3.98 (t, $J = 5.5$ Hz, $0.54 \times 2\text{H}$), 2.83 (t, $J = 5.3$ Hz, $0.46 \times 2\text{H}$), 2.73 (t, $J = 5.2$ Hz, $0.54 \times 2\text{H}$), 2.54–2.47 (m, 2H), 2.39 (s, $0.46 \times 6\text{H}$), 2.33 (s, $0.54 \times 6\text{H}$), 0.96–0.92 (m, 3H); ^{13}C NMR (125 MHz, CD_3OD) δ 165.7, 163.6, 163.5, 159.2, 158.4, 150.2, 147.7, 147.5, 144.5, 143.58, 143.56, 143.50, 141.1, 139.6, 139.5, 139.3, 137.0, 136.8, 133.9, 133.5, 133.2, 132.9, 132.5, 131.9, 131.1, 130.96, 130.95, 129.2, 129.1, 128.8, 128.0, 127.6, 127.5, 120.5, 115.5, 114.7, 114.1, 66.5, 66.2, 59.2, 59.1, 49.8, 49.7, 45.9, 45.8, 30.2, 30.1, 14.1, 14.0; LRMS(ESI^+) m/z calcd for $\text{C}_{33}\text{H}_{35}\text{N}_4\text{O}_3$ [$\text{M} + \text{H}$] $^+$ 535.27; found 535.17.

Characterization of Compound B5: ^1H NMR (500 MHz, DMSO- d_6) δ 11.96 (br s, 1H), 11.54 (br s, 1H), 8.33 (br s, 1H), 8.16 (s, 1H), 7.93 (dd, $J = 9.7, 2.3$ Hz, 1H), 7.72–7.67 (m, 4H), 7.62 (d, $J = 7.5$ Hz, 2H), 7.39 (t, $J = 7.5$ Hz, 2H), 7.35–7.26 (m, 3H), 6.41 (d, $J = 9.5$ Hz, 1H); ^{13}C NMR (125 MHz, DMSO- d_6) δ 161.9, 138.5, 136.7, 133.3, 129.39, 129.35, 129.3, 128.4, 127.62, 127.57, 127.57, 127.48, 127.0, 126.6, 126.3, 118.9, 118.8, 111.0; LRMS(APCI $^+$) m/z calcd for $\text{C}_{21}\text{H}_{18}\text{N}_3\text{O}_2$ [$\text{M} + \text{H}$] $^+$ 344.14; found 344.15.

Characterization of Compound B6: ^1H NMR (500 MHz, DMSO- d_6) δ 12.15 (br s, 1H), 11.82 (s, 1H), 8.45 (s, 1H), 8.17 (s, 1H), 7.98–7.89 (m, 7H), 7.63–7.57 (m, 3H), 6.43 (d, $J = 9.5$ Hz, 1H); ^{13}C NMR (125 MHz, DMSO- d_6) δ

162.4, 160.5, 152.4, 152.0, 145.8, 139.2, 138.2, 137.2, 131.9, 129.6, 128.1, 123.2, 122.7, 119.5, 111.0; LRMS(APCI⁺) *m/z* calcd for C₁₉H₁₆N₅O₂ [M + H]⁺ 346.13; found 346.07.

Characterization of Compound C1: ¹H NMR (500 MHz, CD₃OD) δ 8.42 (s, 1H), 8.22 (s, 1H), 7.99 (dd, *J* = 9.3, 1.8 Hz, 1H), 7.70 (d, *J* = 7.5 Hz, 2H), 7.28 (d, *J* = 8.0 Hz, 2H), 6.55 (d, *J* = 9.5 Hz, 1H), 3.61 (s, 3H), 2.90 (quin, *J* = 7.0 Hz, 1H), 1.25 (d, *J* = 7.0 Hz, 6H); ¹³C NMR (125 MHz, CD₃OD) δ 165.0, 163.3, 153.2, 150.4, 143.8, 139.5, 133.1, 129.0, 127.9, 119.5, 113.9, 38.7, 35.4, 24.2; LRMS(APCI⁺) *m/z* calcd for C₁₇H₂₀N₃O₂ [M + H]⁺ 298.16; found 298.07.

Characterization of Compound C2: ¹H NMR (500 MHz, CD₃OD) δ 8.32 (d, *J* = 2.5 Hz, 1H), 8.07 (s, 1H), 7.94 (dd, *J* = 9.5, 2.5 Hz, 1H), 7.52 (d, *J* = 9.0 Hz, 2H), 6.62 (d, *J* = 8.5 Hz, 2H), 6.49 (d, *J* = 9.5 Hz, 1H), 3.55 (s, 3H), 3.37 (q, *J* = 7.2 Hz, 4H), 1.13 (t, *J* = 7.0 Hz, 6H); ¹³C NMR (125 MHz, CD₃OD) δ 165.0, 162.9, 151.7, 151.1, 143.5, 139.7, 130.8, 121.8, 119.5, 114.3, 112.3, 45.5, 38.8, 13.1; LRMS(APCI⁺) *m/z* calcd for C₁₈H₂₃N₄O₂ [M + H]⁺ 327.18; found 327.19.

Characterization of Compound C3: a mixture of stereoisomers (*E/Z* = 36: 64); ¹H NMR (500 MHz, acetone-*d*₆) δ 8.43 (br s, 1H), 7.98 (s, 0.64 \times 1H), 7.94 (s, 0.36 \times 1H), 7.77 (d, *J* = 7.0 Hz, 0.64 \times 2H), 7.46–6.97 (m, 0.64 \times 8H, 0.36 \times 10H), 6.43 (d, *J* = 9.5 Hz, 0.64 \times 1H), 6.40 (d, *J* = 9.5 Hz, 0.36 \times 1H), 3.60 (s, 0.64 \times 3H), 3.57 (s, 0.36 \times 3H), 2.63–2.60 (m, 0.36 \times 4H), 2.20–2.16 (m, 0.64 \times 4H), 0.99–0.95 (m, 0.36 \times 6H), 0.80–0.77 (m, 0.64 \times 6H); ¹³C NMR (75 MHz, acetone-*d*₆) δ 163.0, 145.6, 144.2, 143.4, 141.2, 140.9, 139.8, 134.2, 131.3, 130.8, 130.3, 129.7, 129.2, 128.7, 128.6, 128.32, 128.25, 128.1, 127.5, 127.4, 127.2, 126.8, 119.4, 112.7, 38.0, 37.98, 28.2, 27.9, 27.6, 27.3, 13.7, 13.63, 13.58, 9.9; LRMS(APCI⁺) *m/z* calcd for C₂₆H₂₈N₃O₂ [M + H]⁺ 414.22; found 414.16.

Characterization of Compound C4: a mixture of stereoisomers (*E/Z* = 45: 55); ¹H NMR (500 MHz, CD₃OD) δ 8.45 (s, 0.55 \times 1H), 8.39 (s, 0.45 \times 1H), 8.29 (s, 0.55 \times 1H), 8.10 (s, 0.45 \times 1H), 8.00 (d, *J* = 9.0 Hz, 0.55 \times 1H), 7.95 (d, *J* = 9.0 Hz, 0.45 \times 1H), 7.77 (d, *J* = 7.5 Hz, 0.55 \times 2H), 7.40 (d, *J* = 8.0 Hz, 0.45 \times 2H), 7.26 (d, *J* = 8.0 Hz, 0.55 \times 2H), 7.27–7.07 (m, 0.55 \times 5H, 0.45 \times 7H), 6.94 (d, *J* = 8.5 Hz, 0.45 \times 2H), 6.90 (d, *J* = 8.5 Hz, 0.45 \times 2H), 6.76 (d, *J* = 8.5 Hz, 0.55 \times 2H), 6.58 (d, *J* = 9.0 Hz, 0.55 \times 2H), 6.54–6.51 (m, 1H), 4.11 (t, *J* = 5.5 Hz, 0.45 \times 2H), 3.93 (t, *J* = 5.2 Hz, 0.55 \times 2H), 3.60 (s, 0.55 \times 3H), 3.57 (s, 0.45 \times 3H), 2.77 (t, *J* = 5.5 Hz, 0.45 \times 2H), 2.66 (t, *J* = 5.5 Hz, 0.55 \times 2H), 2.52–2.44 (m, 2H), 2.34 (s, 0.45 \times 6H), 2.27 (s, 0.55 \times 6H), 0.93–0.90 (m, 3H); ¹³C NMR (125 MHz, CD₃OD) δ 165.05, 165.02, 163.5, 163.4, 159.3, 158.5, 150.3, 150.2, 147.7, 147.5, 144.5, 143.96, 143.89, 143.6, 143.5, 139.68, 139.64, 139.5, 139.4, 137.0, 136.7, 133.9, 133.2, 132.9, 132.5, 131.9, 131.1, 130.97, 130.95, 129.2, 129.1, 128.8, 128.0, 127.6, 127.5, 119.7, 119.6, 115.5, 114.7, 114.04, 114.00, 66.7, 66.5, 59.3, 59.2, 46.02, 45.96, 38.8, 30.2, 30.1, 14.1, 14.0; LRMS (APCI⁺) *m/z* calcd for C₃₄H₃₈N₄O₃ [M + H]⁺ 550.29; found 550.12.

Characterization of Compound C5: ¹H NMR (500 MHz, DMSO-*d*₆) δ 11.64 (s, 1H), 8.48 (s, 1H), 8.36 (s, 1H), 7.93

(dd, *J* = 9.5, 2.0 Hz, 1H), 7.72–7.69 (m, 4H), 7.63 (d, *J* = 8.0 Hz, 2H), 7.41–7.28 (m, 5H), 6.47 (d, *J* = 9.5 Hz, 1H), 3.53 (s, 3H); ¹³C NMR (125 MHz, CD₃OD) δ 161.8, 160.3, 146.8, 142.9, 138.8, 137.8, 136.9, 133.4, 129.6, 128.8, 128.0, 127.8, 127.5, 127.0, 126.7, 118.0, 111.2, 37.5; LRMS(ESI⁺) *m/z* calcd for C₂₂H₂₀N₃O₂ [M + H]⁺ 358.16; found 358.05.

Characterization of Compound C6: ¹H NMR (500 MHz, DMSO-*d*₆) δ 11.82 (s, 1H), 8.51 (s, 1H), 8.44 (s, 1H), 7.99–7.91 (m, 7H), 7.64–7.57 (m, 3H), 6.48 (d, *J* = 9.5 Hz, 1H), 3.53 (s, 3H); ¹³C NMR (125 MHz, CD₃OD) δ 161.8, 160.4, 152.4, 152.0, 145.9, 143.1, 137.8, 137.1, 131.9, 129.6, 128.1, 123.2, 122.7, 118.1, 111.1, 37.5; LRMS(APCI⁻) *m/z* calcd for C₂₀H₁₆N₅O₂ [M - H]⁻ 358.16; found 358.03.

Characterization of Compound D1: ¹H NMR (500 MHz, CD₃OD) δ 8.26 (s, 1H), 7.73–7.70 (m, 4H), 7.28 (d, *J* = 8.0 Hz, 2H), 6.70 (dd, *J* = 7.0, 2.0 Hz, 2H), 2.92 (quin, *J* = 7.0 Hz, 1H), 1.25 (d, *J* = 6.5 Hz, 6H); ¹³C NMR (125 MHz, CD₃OD) δ 167.3, 154.1, 152.9, 149.5, 133.6, 130.7, 129.0, 128.0, 121.3, 114.8, 35.6, 24.4; LRMS(APCI⁺) *m/z* calcd for C₁₇H₂₀N₃O [M + H]⁺ 282.16; found 282.08.

Characterization of Compound D2: ¹H NMR (500 MHz, CD₃OD) δ 8.14 (s, 1H), 7.70 (d, *J* = 8.5 Hz, 2H), 7.62 (d, *J* = 8.5 Hz, 2H), 6.70 (d, *J* = 8.5 Hz, 4H), 3.43 (q, *J* = 7.2 Hz, 4H), 1.18 (t, *J* = 7.0 Hz, 6H); ¹³C NMR (125 MHz, CD₃OD) δ 167.0, 153.8, 151.0, 150.8, 130.7, 130.5, 122.4, 121.7, 114.9, 112.5, 45.5, 13.1; LRMS(APCI⁺) *m/z* calcd for C₁₈H₂₃N₄O [M + H]⁺ 311.19; found 311.08.

Characterization of Compound D3: a mixture of stereoisomers (*E/Z* = 59:41); ¹H NMR (500 MHz, acetone-*d*₆) δ 10.75 (s, 0.41 \times 1H), 10.64 (s, 0.59 \times 1H), 8.47 (s, 0.41 \times 1H), 8.28 (s, 0.59 \times 1H), 7.81–7.74 (m, 3H), 7.44–7.39 (m, 2H), 7.32–7.26 (m, 2H), 7.09–6.97 (m, 4H), 6.74–6.68 (m, 2H), 5.28–5.23 (m, 2H), 2.64–2.58 (m, 0.59 \times 4H), 2.21–2.16 (m, 0.41 \times 4H), 0.99–0.94 (m, 0.59 \times 6H), 0.80–0.76 (m, 0.41 \times 6H); ¹³C NMR (125 MHz, acetone-*d*₆) δ 152.9, 145.8, 144.9, 144.0, 143.2, 140.8, 140.5, 139.71, 139.65, 134.5, 133.5, 131.0, 130.6, 130.2, 130.0, 129.6, 129.1, 128.5, 127.8, 127.4, 127.1, 126.7, 122.2, 114.0, 29.3, 29.0, 28.1, 27.8, 13.7, 13.65, 13.59, 13.56; LRMS(APCI⁺) *m/z* calcd for C₂₆H₂₈N₃O [M + H]⁺ 398.22; found 398.33.

Characterization of Compound D4: a mixture of stereoisomers (*E/Z* = 45:55); ¹H NMR (500 MHz, CD₃OD) δ 8.31 (s, 0.55 \times 1H), 8.12 (s, 0.45 \times 1H), 7.80 (d, *J* = 8.0 Hz, 0.55 \times 2H), 7.74 (d, *J* = 8.5 Hz, 0.55 \times 2H), 7.69 (d, *J* = 8.5 Hz, 0.45 \times 2H), 7.43 (d, *J* = 8.0 Hz, 0.45 \times 2H), 7.26 (d, *J* = 8.0 Hz, 0.55 \times 2H), 7.17–7.07 (m, 0.55 \times 5H, 0.45 \times 7H), 6.94 (d, *J* = 8.5 Hz, 0.45 \times 2H), 6.89 (d, *J* = 8.0 Hz, 0.45 \times 2H), 6.76 (d, *J* = 9.0 Hz, 0.55 \times 2H), 6.71 (d, *J* = 8.5 Hz, 0.55 \times 2H), 6.68 (d, *J* = 8.5 Hz, 0.45 \times 2H), 6.58 (d, *J* = 9.0 Hz, 0.55 \times 2H), 4.10 (t, *J* = 5.2 Hz, 0.45 \times 2H), 3.93 (t, *J* = 5.5 Hz, 0.55 \times 2H), 2.76 (t, *J* = 5.2 Hz, 0.45 \times 2H), 2.66 (t, *J* = 5.5 Hz, 0.55 \times 2H), 2.52–2.45 (m, 2H), 2.34 (s, 0.46 \times 6H), 2.27 (s, 0.54 \times 6H), 0.94–0.91 (m, 3H); ¹³C NMR (125 MHz, CD₃OD) δ 167.3, 167.2, 159.3, 158.4, 154.2, 154.1, 149.2, 149.1, 147.3, 147.1, 144.4, 143.64, 143.57, 143.5, 139.58, 139.46, 137.1, 136.8, 134.4, 133.3, 133.2, 132.4, 131.9, 131.1, 130.98, 130.76, 130.69, 129.17, 129.11, 128.7, 127.9, 127.6, 127.4, 121.1, 115.5,

114.79, 114.75, 114.66, 66.7, 66.5, 59.3, 59.2, 46.0, 45.9, 30.2, 30.1, 14.1, 14.0; LRMS(APCI⁺) *m/z* calcd for C₃₄H₃₇N₄O₂ [M + H]⁺ 533.29; found: 533.11.

Characterization of Compound D5: ¹H NMR (500 MHz, DMSO-*d*₆) δ 11.47 (s, 1H), 8.40 (s, 1H), 7.71–7.66 (m, 6H), 7.63 (d, *J* = 7.5 Hz, 2H), 7.41–7.27 (m, 5H), 6.61 (d, *J* = 8.5 Hz, 2H), 5.78 (s, 2H); ¹³C NMR (75 MHz, DMSO-*d*₆) δ 163.0, 152.3, 145.5, 138.4, 136.9, 133.9, 129.4, 128.8, 127.9, 127.2, 126.9, 126.6, 119.4, 112.6; LRMS(APCI⁺) *m/z* calcd for C₂₂H₂₀N₃O [M + H]⁺ 342.16; found 342.26.

Characterization of Compound D6: ¹H NMR (500 MHz, DMSO-*d*₆) δ 11.63 (s, 1H), 8.48 (br s, 1H), 7.98–7.91 (m, 6H), 7.70 (d, *J* = 8.5 Hz, 2H), 7.63–7.57 (m, 5H), 6.61 (d, *J* = 8.5 Hz, 2H), 5.83 (s, 2H); ¹³C NMR (125 MHz, DMSO-*d*₆) δ 152.4, 152.2, 152.0, 137.7, 131.7, 129.5, 127.8, 123.2, 122.6, 119.3, 112.6; LRMS(ESI⁺) *m/z* calcd for C₂₀H₁₈N₅O [M + H]⁺ 344.15; found 344.26.

Characterization of Compound E1: ¹H NMR (300 MHz, CD₃OD) δ 8.55 (s, 1H), 8.27 (s, 1H), 7.99 (d, *J* = 7.5 Hz, 1H), 7.74 (d, *J* = 7.4 Hz, 2H), 7.30 (d, *J* = 8.0 Hz, 2H), 6.62 (d, *J* = 8.8 Hz, 1H), 2.94 (quin, *J* = 6.9 Hz, 1H), 1.27 (d, *J* = 6.9 Hz, 6H); ¹³C NMR (125 MHz, CD₃OD) δ 165.4, 163.2, 153.0, 150.0, 149.5, 138.4, 133.3, 128.9, 127.9, 118.3, 109.2, 35.4, 24.2; LRMS(ESI⁺) *m/z* calcd for C₁₆H₁₉N₄O [M + H]⁺ 283.16; found 283.17.

Characterization of Compound E2: ¹H NMR (300 MHz, DMSO-*d*₆) δ 11.19 (s, 1H), 8.51 (s, 1H), 8.22 (s, 1H), 7.86 (d, *J* = 8.1 Hz, 1H), 7.47 (d, *J* = 8.1 Hz, 2H), 6.70 (d, *J* = 8.7 Hz, 2H), 6.52 (s, 2H), 6.46 (d, *J* = 8.7 Hz, 2H), 3.38 (q, *J* = 6.9 Hz, 4H), 1.11 (t, *J* = 6.9 Hz, 6H); ¹³C NMR (125 MHz, CD₃OD) δ 163.2, 151.5, 151.3, 149.4, 138.4, 130.7, 122.4, 119.1, 112.67, 112.64, 109.4, 45.5, 13.0; LRMS(ESI⁺) *m/z* calcd for C₁₇H₂₂N₅O [M + H]⁺ 312.18; found 312.11.

Characterization of Compound E3: a mixture of stereoisomers (*E/Z* = 75:25); ¹H NMR (500 MHz, acetone-*d*₆) δ 8.68 (s, 0.25 × 1H), 8.63 (s, 0.75 × 1H), 7.96 (d, *J* = 6.0, 0.75 × 1H), 7.78 (d, *J* = 8.0, 0.75 × 1H), 7.44–7.26 (m, 3H), 7.09–6.98 (m, 5H), 6.61 (d, *J* = 9.0, 0.25 × 1H), 6.58 (d, *J* = 8.5, 0.75 × 1H), 5.99 (s, 2H), 2.64–2.58 (m, 0.75 × 4H), 2.21–2.16 (m, 0.25 × 4H), 0.99–0.94 (m, 0.75 × 6H), 0.80–0.77 (m, 0.41 × 6H); ¹³C NMR (125 MHz, acetone-*d*₆) δ 146.0, 144.0, 143.2, 140.9, 139.7, 139.6, 131.1, 130.7, 130.1, 129.6, 129.1, 128.5, 127.9, 127.4, 127.2, 126.7, 119.2, 107.8, 28.1, 27.8, 13.7, 13.6; LRMS(APCI⁺) *m/z* calcd for C₂₅H₂₇N₄O [M + H]⁺ 399.22; found 399.28.

Characterization of Compound E4: a mixture of stereoisomers (*E/Z* = 45:55); ¹H NMR (500 MHz, CD₃OD) δ 8.56 (s, 0.55 × 1H), 8.51 (s, 0.45 × 1H), 8.32 (s, 0.55 × 1H), 8.13 (s, 0.45 × 1H), 7.99 (dd, *J* = 9.0, 2.0 Hz, 0.55 × 1H), 7.94 (dd, *J* = 8.8, 1.7 Hz, 0.45 × 1H), 7.81 (d, *J* = 8.0 Hz, 0.55 × 2H), 7.44 (d, *J* = 8.0 Hz, 0.45 × 2H), 7.27 (d, *J* = 8.0 Hz, 0.55 × 2H), 7.18–7.08 (m, 7H), 6.96 (d, *J* = 8.5 Hz, 0.45 × 2H), 6.91 (d, *J* = 8.0 Hz, 0.45 × 2H), 6.78 (d, *J* = 8.5 Hz, 0.55 × 2H), 6.63–6.58 (m, 2H), 4.14 (t, *J* = 5.5 Hz, 0.45 × 2H), 3.98 (t, *J* = 5.3 Hz, 0.55 × 2H), 2.87 (t, *J* = 5.5 Hz, 0.45 × 2H), 2.77 (t, *J* = 5.3 Hz, 0.55 × 2H), 2.53–2.46 (m, 2H), 2.42 (s, 0.45 × 6H), 2.35 (s, 0.55 × 6H), 0.94–0.91 (m, 3H); ¹³C NMR (125 MHz, CD₃OD) δ 165.6, 165.5, 163.41, 163.37, 159.2, 158.4, 149.8, 149.73,

149.67, 147.5, 147.3, 144.5, 143.62, 143.61, 143.55, 139.6, 139.4, 138.53, 138.47, 137.2, 136.9, 134.2, 133.2, 133.1, 132.4, 131.9, 131.1, 131.0, 129.2, 129.1, 128.8, 128.0, 127.6, 127.5, 118.4, 115.5, 114.7, 109.4, 66.4, 66.1, 59.2, 59.1, 45.8, 45.7, 30.2, 30.1, 14.03, 13.99; LRMS(APCI⁺) *m/z* calcd for C₃₃H₃₆N₅O₂ [M + H]⁺ 534.29; found 534.06.

Characterization of Compound E5: ¹H NMR (500 MHz, DMSO-*d*₆) δ 11.58 (br s, 1H), 8.55 (d, *J* = 2.0 Hz, 1H), 8.39 (br s., 1H), 7.89 (dd, *J* = 8.5, 2.5 Hz, 1H), 7.70–7.68 (m, 4H), 7.63 (d, *J* = 7.0 Hz, 2H), 7.41–7.28 (m, 5H), 6.64 (s, 2H), 6.48 (d, *J* = 9.0 Hz, 1H); ¹³C NMR (125 MHz, DMSO-*d*₆) δ 138.5, 136.9, 133.7, 129.4, 128.8, 127.9, 127.8, 127.3, 126.9, 126.6, 116.7, 106.9; LRMS(ESI⁺) *m/z* calcd for C₂₁H₁₉N₄O [M + H]⁺ 343.16; found 343.11.

Characterization of Compound E6: ¹H NMR (500 MHz, DMSO-*d*₆) δ 11.69 (br s, 1H), 8.58 (d, *J* = 2.5 Hz, 1H), 8.47 (br s., 1H), 7.98–7.90 (m, 7H), 7.64–7.57 (m, 7H), 6.61 (s, 2H), 6.50 (d, *J* = 9.0 Hz, 1H); ¹³C NMR (125 MHz, DMSO-*d*₆) δ 161.8, 152.3, 152.0, 149.1, 145.1, 137.4, 136.6, 131.7, 129.5, 127.9, 123.1, 122.6, 116.6, 106.9; LRMS(APCI⁺) *m/z* calcd for C₁₉H₁₇N₆O [M + H]⁺ 345.15; found 345.00.

Supporting Information Available. General procedure for synthesis of hydrazide B–E, synthetic procedure of aldehyde building blocks 3, 4, and 6, ¹H and ¹³C NMR spectra, structural confirmation of *E/Z* isomer of aldehyde 4 (*E/Z* mixture) via 1-dimensional ¹H NOE experiment, and docking test result. This material is available free of charge via the Internet at <http://pubs.acs.org>.

References and Notes

- (1) (a) Olefsky, J. M. *J. Biol. Chem.* **2001**, *276*, 36863–36864. (b) Kliever, S.; Lehmann, J.; Willson, T. *Science* **1999**, *284*, 757–760. (c) Abad, M. C.; Askari, H.; O'Neill, J.; Klinger, A. L.; Milligan, C.; Lewandowski, F.; Springer, B.; Spurlino, J.; Rentzeperis, D. *J. Steroid Biochem. Mol. Biol.* **2008**, *108*, 44–54.
- (2) (a) Germain, P.; Staels, B.; Dacquet, C.; Spedding, M.; Laudet, V. *Pharmacol. Rev.* **2006**, *58*, 685–704. (b) Kumar, R.; Johnson, B.; Thompson, E. *Essays Biochem.* **2004**, *40*, 27–39. (c) Moras, D.; Gronemeyer, H. *Curr. Opin. Cell Biol.* **1998**, *10*, 384–391.
- (3) (a) Giguère, V. *Endocr. Rev.* **1999**, *20*, 689–725. (b) Blumberg, B.; Evans, R. M. *Genes Dev.* **1998**, *12*, 3149–3155.
- (4) Giguère, V.; Yang, N.; Segui, P.; Evans, R. M. *Nature* **1988**, *331*, 91–94.
- (5) Horard, B.; Vanacker, J. *J. Mol. Endocrinol.* **2003**, *31*, 349–357.
- (6) Kraus, R. J.; Ariazi, E. A.; Farrell, M. L.; Mertz, J. E. *J. Biol. Chem.* **2002**, *277*, 24826–24834.
- (7) (a) Eudy, J.; Yao, S.; Weston, M.; Ma-Edmonds, M.; Talmadge, C.; Cheng, J.; Kimberling, W.; Sumegi, J. *Genomics* **1998**, *50*, 382–384. (b) Hong, H.; Yang, L.; Stallcup, M. R. *J. Biol. Chem.* **1999**, *274*, 22618–22626. (c) Heard, D.; Norby, P.; Holloway, J.; Vissing, H. *Mol. Endocrinol.* **2000**, *14*, 382–392.
- (8) Ariazi, E. A.; Clark, G. M.; Mertz, J. E. *Cancer Res.* **2002**, *62*, 6510–6518.
- (9) (a) Brzozowski, A.; Pike, A.; Dauter, Z.; Hubbard, R.; Bonn, T.; Engström, O.; Öhman, L.; Greene, G.; Gustafsson, J.; Carlquist, M. *Nature* **1997**, *389*, 753–758. (b) Tremblay, G.; Bergeron, D.; Giguère, V. *Endocrinology* **2001**, *142*, 4572–4575. (c) Tremblay, G. B.; Kunath, T.; Bergeron, D.; Lapointe, L.; Champigny, C.; Bader, J.-A.; Rossant, J.; Giguère, V.

Genes Dev. **2001**, *15*, 833–838. (d) Coward, P.; Lee, D.; Hull, M.; Lehmann, J. *Proc. Natl. Acad. Sci.* **2001**, *98*, 8880–8884. (e) allen, J.; Schlaeppli, J.-M.; Bitsch, F.; Filipuzzi, I.; Schilb, A.; Riou, V.; Graham, A.; Strauss, A.; Geiser, M.; Fournier, B. *J. Biol. Chem.* **2004**, *279*, 49330–49337. (f) Greschik, H.; Wurtz, J.; Sanglier, S.; Bourguet, W.; van Dorsselaer, A.; Moras, D.; Renaud, J. *Mol. Cell* **2002**, *9*, 303–313. (g) Greschik, H.; Flaig, R.; Renaud, J.-P.; Moras, D. *J. Biol. Chem.* **2004**, *279*, 33639–33646.

- (10) Zuercher, W. J.; Gaillard, S.; Orband-Miller, L. A.; Chao, E. Y. H.; Shearer, B. G.; Jones, D. G.; Miller, A. B.; Collins, J. L.; McDonnell, D. P.; Willson, T. M. *J. Med. Chem.* **2005**, *48*, 3107–3109.
 - (11) Wang, L.; Zuercher, W. J.; Consler, T. G.; Lambert, M. H.; Miller, A. B.; Orband-Miller, L. A.; McKee, D. D.; Willson, T. M.; Nolte, R. T. *J. Biol. Chem.* **2006**, *281*, 37773–37781.
 - (12) Sadowski, I.; Ptashne, M. *Nucleic Acids Res.* **1989**, *17*, 7539.
- CC900081J